Xiaoping Liu
Graduate Programs in Manufacturing Systems Engineering,
University of St. Thomas,
St. Paul, MN 55105

R. D. James[1]
Department of Aerospace Engineering and Mechanics,
University of Minnesota,
110 Union Street, S.E.,
Minneapolis, MN 55455

Stability of Fiber Networks Under Biaxial Stretching

This paper is concerned with the constitutive behavior of a particular orthogonal fiber network under biaxial dead loading. We also describe a new kind of biaxial, dead-loading machine which is applicable to anisotropic materials. The machine does not require that the loads are exerted along symmetry axes of the material. A specimen of the cloth was loaded by different loading paths to the same equibiaxial dead-load, and two different final deformations were observed. A related observation was reported by Treloar for rubber in 1948. In order to understand this instability, we experimentally determined the energy function for the cloth. The energy function is then used in a variational calculation to explain this instability.

1 Introduction

In this paper we introduce a new biaxial testing machine that imposes approximately uniform dead-load tractions to the edges of a plate, and we study the deformation of cloth. The machine is applicable to anisotropic materials, which may undergo large deformations, and the tractions need not be imposed along symmetry axes of the material.

To test the ability of the machine to accurately impose these tractions, we placed in the machine an extremely anisotropic material which also easily undergoes large deformations, this being a sample of Kevlar® parachute cloth with a relatively open orthogonal weave. Usually we found that an assignment of the two resultant forces yielded a unique homogeneous deformation, regardless of the loading path. The homogeneity of this deformation and the independence of the loading path are quantified in Section 4. However, when we loaded to an equibiaxial load, we observed that the final deformation was not unique. More specially, we found that associated to each equibiaxial load there are precisely two homogeneous deformations, and the observed deformation is always near one of these, although there is some scatter (see Section 4). This nonuniqueness admits a simple interpretation based on symmetry and nonlinearity (Section 5).

To explain these observations, we settled on a simple model for the cloth. We noted that, while the cloth behaves in a highly inelastic manner under small forces, it becomes highly elastic, except for the aforementioned instability, under a large range of biaxial tensions of sufficient magnitude. It is also approximately inextensible in fiber directions. We therefore model the cloth as an inextensible nonlinear elastic material, in the spirit of Pipkin and Rivlin (Pipkin, 1974 and 1987; Pipkin and Rivlin, 1963; Rivlin, 1955) (Section 6). We use the experimental measurements of Piola-Kirchhoff stress versus deformation gradient to evaluate the energy function for the cloth. The resulting energy function exhibits potential wells. Because the experimental data leave gaps in the domain of the energy function, due to the equibiaxial instability, we are not able to uniquely assign a potential well structure to the energy function in all of its domain, but we suggest several reasonable alternatives (Section 7).

A related observation for rubber was reported by Treloar (1948). He carried out an experiment in which a rectangular sheet of rubber was subjected to equal dead-load tensions at its edges. In some cases the resulting deformations were asymmetric, with unequal principal stretches even though the loading was symmetric. At about the same time, Rivlin (1948) studied equilibrium deformations of a cube of neo-Hookean material subjected to three pairs of equal and opposite dead-load surface tractions. He showed that at least seven equilibrium configurations are possible when the tensile forces exceed a certain critical value, and of the seven, only one has all the symmetries of the given loading. Furthermore, he found that the symmetric configuration is unstable for large values of the tensile forces (Rivlin, 1974). Ball and Schaeffer (1983) considered the same problem for general isotropic incompressible materials. Kearsley (1986), MacSithigh (1986), and Chen (1987) also studied the similar problem for isotropic incompressible elastic materials, and some stability approaches have been employed to explain Treloar's observations. A difference between the results of these analyses and the behavior of the cloth studied in this paper is that they predict an infinite number of stable deformations while in the cloth we observe only two.

[1]To whom all correspondence should be addressed.

Contributed by the Applied Mechanics Division of THE AMERICAN SOCIETY OF MECHANICAL ENGINEERS for publication in the ASME JOURNAL OF APPLIED MECHANICS.

Discussion on this paper should be addressed to the Technical Editor, Professor Lewis T. Wheeler, Department of Mechanical Engineering, University of Houston, Houston, TX 77204-4792, and will be accepted until four months after final publication of the paper itself in the ASME JOURNAL OF APPLIED MECHANICS.

Manuscript received by the ASME Applied Mechanics Division, July 1, 1993; final revision, Nov. 4, 1993. Associate Technical Editor: R. Abeyaratne.

2 Preliminaries and Notation

In this section we describe the terminology used for describing the deformation and energy function of the cloth. We consider a body which can be represented in a fixed reference configuration by a bounded regular domain $R \in \mathbb{R}^2$. A particle of the body is represented by $\mathbf{x} \in R$. To formulate constitutive relations for the material, we first define the deformation. A deformation $\mathbf{y}$ is an invertible function

$$\mathbf{y}: R \to \mathbf{y}(R) \tag{1}$$

which maps the reference shape R onto the present shape $\mathbf{y}(R) \in \mathbb{R}^2$. We assume $\mathbf{y}$ is differentiable at $\mathbf{x} \in R$, we call

$$\mathbf{F} = \nabla \mathbf{y}(\mathbf{x}), \tag{2}$$

the deformation gradient at $\mathbf{x}$. We shall assume throughout this paper, in addition to the invertibility of $\mathbf{y}$, that the deformation gradient satisfies

$$\det \mathbf{F} > 0. \tag{3}$$

In view of our assumption (3), the tensor $\mathbf{F}$ has the unique decomposition:

$$\mathbf{F} = \mathbf{RU} \tag{4}$$

where $\mathbf{U}$ is a positive-definite symmetric tensor called the *stretch* and $\mathbf{R}$ is a proper orthogonal tensor called the *rotation*.

Later we shall assume that the cloth specimen is a homogeneous elastic material which possesses a strain-energy function φ depending on the local change of shape:

$$\varphi(\mathbf{F}). \tag{5}$$

The value of the strain-energy function $\varphi(\mathbf{F})$ corresponds to the strain energy, per unit area in the reference configuration, stored in the body when it undergoes a deformation with the deformation gradient $\mathbf{F}$. The strain-energy function is assumed to satisfy the condition of material frame indifference,

$$\varphi(\mathbf{RF}) = \varphi(\mathbf{F}), \tag{6}$$

$\mathbf{R}$ being any proper orthogonal tensor in two-dimensional space. According to standard continuum mechanics (Chadwick, 1976), if $\mathbf{H}$ is a rotation which belongs to the material symmetry group, φ satisfies

$$\varphi(\mathbf{FH}) = \varphi(\mathbf{F}) \tag{7}$$

for all admissible $\mathbf{F}$. We shall use the notation $\mathbf{H}(\theta)$ to denote a clockwise rotation through the angle θ.

The assumption (6) implies that φ can be expressed as a function of $\mathbf{F}^T\mathbf{F}$ only:

$$\varphi(\mathbf{F}) = \bar{\varphi}(\mathbf{C}), \quad \mathbf{C} = \mathbf{F}^T\mathbf{F}. \tag{8}$$

Let $\mathbf{t}$ represent the force per unit reference length applied to the boundary ∂R of the specimen, which we call the traction, and s the length measure of the boundary. The physical interpretation of a *dead-loading* device is that the imposed force $\mathbf{t}(\mathbf{x})ds$ applied at $\mathbf{y}(\mathbf{x})$ maintains its magnitude and direction regardless of how the body deforms. The design of the machine is such as to impose a dead-load traction $\mathbf{t}(\mathbf{x})$ of the form

$$\mathbf{t}(\mathbf{x}) = \mathbf{Tn}(\mathbf{x}),$$

where $\mathbf{n}(\mathbf{x})$ is the unit normal to ∂R at $\mathbf{x}$ and $\mathbf{T} = \sum_{i=1}^{2} T_i \mathbf{e}_i \otimes \mathbf{e}_i$, where T_1, T_2 are constants and $\mathbf{e}_1$, $\mathbf{e}_2 \in \mathbb{R}^2$ are orthogonal. In the equibiaxial case $T_1 = T_2$.

The total potential energy $E[\mathbf{y}]$ of a dead-loaded body is defined by

$$E[\mathbf{y}] = \int_R \varphi(\nabla \mathbf{y}(\mathbf{x}))d\mathbf{x} - \int_{\partial R} \mathbf{t}(\mathbf{x}) \cdot \mathbf{y}(\mathbf{x})ds. \tag{9}$$

Given a traction field $\mathbf{t}(\mathbf{x})$, a deformation $\mathbf{y}^*(\mathbf{x})$ is stable in a dead loading device, if it minimizes the total potential energy; the inequality

$$E[\mathbf{y}^*] \le E[\mathbf{y}] \tag{10}$$

holds for all admissible deformations $\mathbf{y}$. For our purposes, the set of admissible deformations will be all smooth deformations whose gradient lies in the domain of the function φ.

3 The Testing Machine and Specimen

By looking at the reports available in literature on biaxial loading experiments, we found that two test devices were reported in early days. Treloar (1949) designed a series of experiments using vulcanized natural rubber to test the applicability of the neo-Hooken form of the strain-energy function. Among his experiments, there was a biaxial test machine, which stretched a thin square sheet of rubber. In Treloar's experiment the square test-piece had five projecting lugs on each side as indicated schematically in Fig. 1, and strings were tied to these for the application of loads. The surface of the sheet was marked out with lines forming a square lattice. With the sheet placed horizontally, the three middle lugs on a side were loaded by means of three equal weights attached to each string, while the strings attached to the two outermost lugs were secured to a rectangular frame.

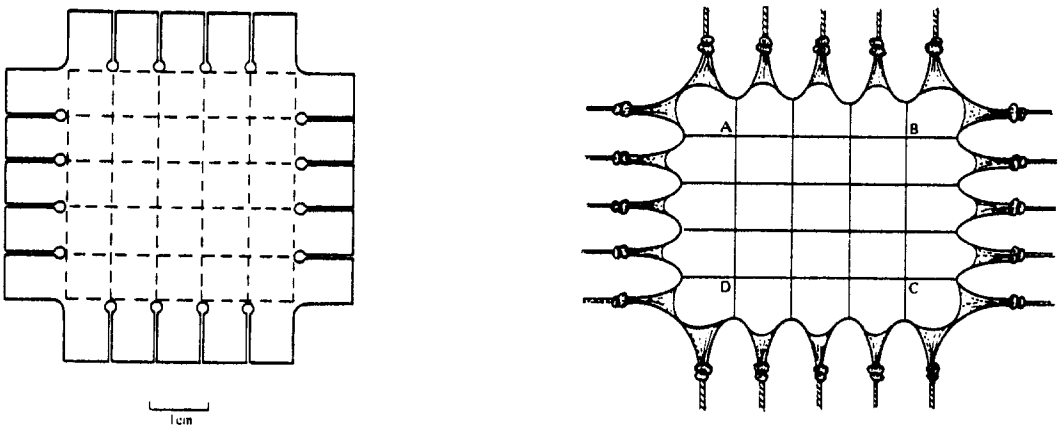

Fig. 1 From Treloar, 1958 (With permission from R. J. Atkin and N. Fox, *An Introduction to the Theory of Elasticity*, Fig. 3.6 and 3.7, Longman, London and New York, 1980)

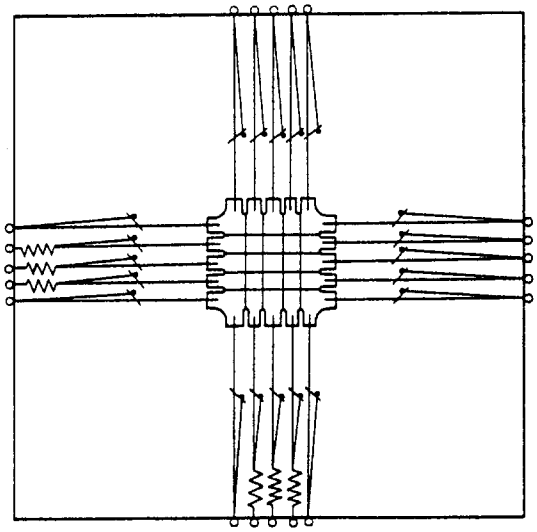

Fig. 2 Experimental set-up of Rivlin and Saunders, 1951 (With permission from R. J. Atkin and N. Fox, *An Introduction to the Theory of Elasticity*, Fig. 3.9, Longman, London and New York, 1980)

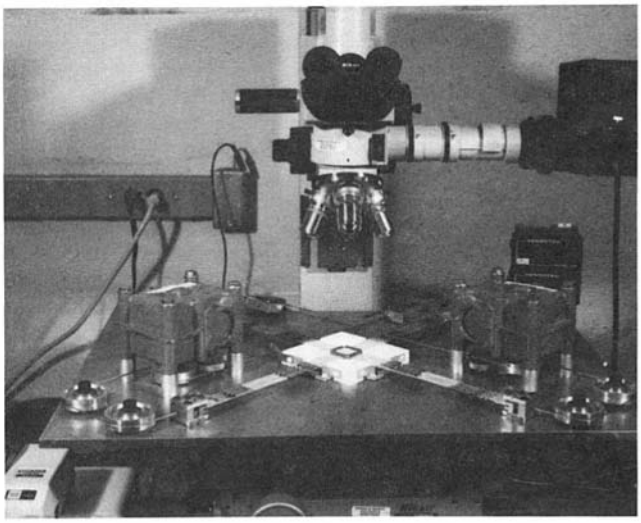

Fig. 3 A view of the loading arrangement of the biaxial machine

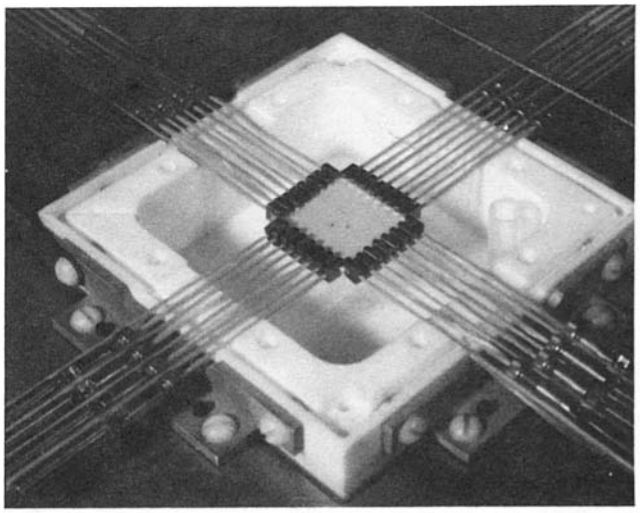

Fig. 4 A view of the environment chamber and specimen

Similar arrangements were used on the other three sides, and by applying different weights, different extensions were obtained. The appearance of the stretched sheet is shown in Fig. 1. By measuring the lengths of the sides of rectangles drawn on the sheet in their deformed and undeformed states, he determined the principal stretches. In the experiment it was assumed that the traction operative in producing the pure homogeneous deformation of the rectangle ABCD was computed from the loads applied to the three central lugs on each side of the test piece.

Rivlin and Saunders (1951) used the arrangement shown in Fig. 2. One difference between their arrangement and that of Treloar's is that springs were used instead of weights, so that rapid, continuous variation of the applied traction was possible. Again it was assumed that the traction operative in producing the pure homogeneous deformation of the central nine squares was computed from the central three strings on each side of the test piece.

When the material shears, the line connecting the loading points rotates relative to the direction of the applied force. In this case Treloar and Rivlin and Saunders' machines will give a nonuniform load distribution. This fact makes their machines inapplicable to the testing of anisotropic materials. Secondly, the five loading points on each side of the specimen seem insufficient to approximate a uniform load distribution. Additionally, with modern instrumentation and a high precision X-Y table it is possible to get more accurate measurements.

Our biaxial dead loading machine is pictured in Figs. 3 and 4 and is described in detail as follows. The standard specimens are thin square sheets of approximate dimensions 3.175 cm with eight epoxy dots on each edge. Eight C-clamps or grips are fastened to each edge. Each grip is fastened to the specimen by two #0 − 80 screws, one from above and one from below. This construction allows each grip to pivot on the epoxy dot. Each of the 32 grips is in turn attached via Kevlar® fibers to a soft spring. The function of the spring is to keep the force in Kevlar® fibers relatively uniform. Hence, there are four sets of eight fibers attached to the edges of the specimen, one set or "group" per side. The ends of each group of fibers are linearly fastened to a steel arm which is encased in a housing which allows the entire set of fibers to pivot. This arrangement has the property that the steel arm will turn so as to equalize, on average, the forces in the fibers.

The arm is attached to a steel tensioning cable. After a 180 deg change of direction through the utilization of a companion pair of pulleys, the cable is attached to a 60:1 worm reducer. There is one worm reducer for each axis of the specimen. This arrangement forms a closed loop (i.e., specimen-fiber-reducer-fiber-specimen) so that the force produced along each edge is equal to the force produced on its opposing edge. This also allows the resultant force on each axis to be measured by a load cell which is attached to one of the cables for each axis. To change the force along either axis, one must only adjust the knob on the appropriate reducer, which in turn drives a disk around which the cable is wound. This process lengthens or shortens the springs attached to the fibers, thus increasing or decreasing the applied force.

This construction of fibers, springs, arms, cables, pulleys, load cells, and reducers constitutes our biaxial dead loading testing machine. Its components are mounted on a precisely machined, high-strength aluminum plate ensuring that accurate and appropriate geometrical positioning of these parts is achieved. The plate is in turn mounted on the X-Y table of an optical microscope. The microscope is equipped with a movable stage which can be positioned through the use of two independent controls: one for the X-axis and one for the

Y-axis. These axial controls are wired to a Metronics Quadra-Chek II which allows the operator to monitor the stage's X and Y coordinates (± 0.00013 cm resolution, 0.0005 cm accuracy) relative to an arbitrarily set origin. We obtained the deformation gradient by measuring the coordinates of three noncollinear markers on the specimen both before and after deformation.

In addition, the load cells are wired to two independent Sensotec load monitors (± 0.0445 N resolution), one for each of the specimen's axes. The arrangement allows the operator of the microscope access to his position of observation and the loads applied to the specimen.

The material studied was supplied by the Fibers Development Center, DuPont Company, Wilmington, DE. The fabric was woven from 55 denier Kevlar® and is 3.3 mils thick. The fabric is formed by two perpendicular families of filaments. Thus, we are led to assume that $\mathbf{H}(n\pi/2)$ where n is the integer belongs to the material symmetry group of undistorted cloth.

To make the specimens, we cut the material at an angle θ to the fibers (see Fig. 5). After cutting square specimens, we glued eight dots of epoxy per edge on both the top and bottom of the specimen for a total 32 equidistant points of contact per side. These epoxy dots did not touch each other. Next, a grip was fastened to each pair of epoxy contact points by two tiny screws, as described above. This allowed the force applied to the edge to be approximately uniform without damaging the specimen. The square defined by the center lines of the screws had dimensions 2.54 cm × 2.54 cm in all cases.

After some preliminary experiments, it was found that another apparatus was needed to aid in attaching the grips with proper alignment. For this purpose we built a device to successively hold the eight grips in their precise location while we systematically attached each side of the cloth to them. This device helped to ensure that the traction force applied to each edge would be uniform.

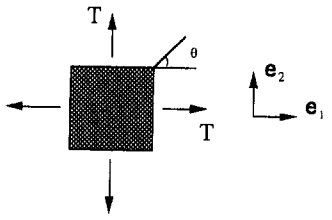

Fig. 5 Notation

4 Experimental Observations

We first conducted a series of experiments to check the homogeneity of the deformations. We randomly chose six points on the specimen, and grouped them in threes. We applied a suitable force in each direction, and measured the coordinates of those six points on the specimen before and after the loading process. According to $\mathbf{dy} = \mathbf{F}\mathbf{dx}$, for each three-point group we can determine a deformation gradient $\mathbf{F}$. In order to quantify the difference between these two deformation gradients, we define $\epsilon = \|\mathbf{F}(2) - \mathbf{F}(1)\|/\|\mathbf{F}(2)\|$, where 1 and 2 represent the group 1 and the group 2 and $\|\mathbf{F}\| = \sqrt{\mathbf{F} \cdot \mathbf{F}}$. Because of the limited accuracy of the x-y table, we kept only the third decimal place in our results. Typically in our tests $\epsilon < 0.004$, so the deformations can be considered nearly homogeneous.

Now we report the observations of instability under equibiaxial tension. First we tested the piece which was cut at $\theta = 22.5$ deg. After we affixed this specimen to the machine, several equibiaxial dead loads were applied, in this case 22.25 N, 26.7 N, 31.5 N, and 35.6 N consecutively. We loaded the force in the $\mathbf{e}_1$ direction first, then loaded to the same force in the $\mathbf{e}_2$ direction. We got a deformation gradient $\mathbf{F}_1$. Next we loaded the force in the $\mathbf{e}_2$ direction first, then loaded the same force in the $\mathbf{e}_1$ direction. We got another deformation gradient $\mathbf{F}_2$. These deformation gradients and corresponding stretch tensors $\mathbf{U}$ and rotation tensors $\mathbf{R}$, are listed in Table 1.

We next tested the fabric by cutting it at an angle $\theta = 35$ deg to the fibers. In exactly the same way, we loaded the forces to 26.7 N and 35.6 N, respectively. We got two sets of $\mathbf{F}$, $\mathbf{U}$ and $\mathbf{R}$. They are listed in Table 2.

When we loaded the specimen, always trying as closely as possible to keep the loads equal during loading, we found that the deformation gradient always adopted a value near those in Table 1 and Table 2 at the corresponding load.

5 Analysis of the Nonuniqueness

The nonuniqueness that is evident from the observation in the equibiaxial case admits the following simple interpretation.

Suppose the observed deformations of the cloth are stable

Table 1

Force	F	U	R
T=22.5 N	$\mathbf{F}_1=\begin{pmatrix} 1.0116 & .0068 \\ .0032 & .9935 \end{pmatrix}$	$\mathbf{U}_1=\begin{pmatrix} 1.0116 & .0050 \\ .0050 & .9935 \end{pmatrix}$	$\mathbf{R}_1=\begin{pmatrix} 1.0000 & .0018 \\ -.0018 & 1.0000 \end{pmatrix}$
	$\mathbf{F}_2=\begin{pmatrix} .9958 & -.0066 \\ -.0031 & 1.0065 \end{pmatrix}$	$\mathbf{U}_2=\begin{pmatrix} .9958 & -.0049 \\ -.0049 & 1.0065 \end{pmatrix}$	$\mathbf{R}_2=\begin{pmatrix} 1.0000 & -.0017 \\ .0017 & 1.0000 \end{pmatrix}$
T = 26.7 N:	$\mathbf{F}_1=\begin{pmatrix} 1.0162 & .0189 \\ .0102 & .9793 \end{pmatrix}$	$\mathbf{U}_1=\begin{pmatrix} 1.0161 & .0146 \\ .0146 & .9794 \end{pmatrix}$	$\mathbf{R}_1=\begin{pmatrix} 1.0000 & .0043 \\ -.0043 & 1.0000 \end{pmatrix}$
	$\mathbf{F}_2=\begin{pmatrix} .9935 & -.0032 \\ -.0068 & 1.0114 \end{pmatrix}$	$\mathbf{U}_2=\begin{pmatrix} .9935 & -.0050 \\ -.0050 & 1.0114 \end{pmatrix}$	$\mathbf{R}_2=\begin{pmatrix} 1.0000 & .0018 \\ -.0018 & 1.0000 \end{pmatrix}$
T=31.5 N	$\mathbf{F}_1=\begin{pmatrix} 1.0062 & .0100 \\ .0032 & .9934 \end{pmatrix}$	$\mathbf{U}_1=\begin{pmatrix} 1.0062 & .0066 \\ .0066 & .9935 \end{pmatrix}$	$\mathbf{R}_1=\begin{pmatrix} 1.0000 & .0034 \\ -.0034 & 1.0000 \end{pmatrix}$
	$\mathbf{F}_2=\begin{pmatrix} .9917 & -.0133 \\ -.0085 & 1.0098 \end{pmatrix}$	$\mathbf{U}_2=\begin{pmatrix} .9916 & -.0108 \\ -.0108 & 1.0098 \end{pmatrix}$	$\mathbf{R}_2=\begin{pmatrix} 1.0000 & -.0015 \\ .0015 & 1.0000 \end{pmatrix}$
T=35.6 N:	$\mathbf{F}_1=\begin{pmatrix} 1.0097 & .0067 \\ .0104 & .9929 \end{pmatrix}$	$\mathbf{U}_1=\begin{pmatrix} 1.0097 & .0085 \\ .0085 & .9928 \end{pmatrix}$	$\mathbf{R}_1=\begin{pmatrix} 1.0000 & -.0019 \\ .0019 & 1.0000 \end{pmatrix}$
	$\mathbf{F}_2=\begin{pmatrix} .9861 & -.0121 \\ -.0092 & 1.0130 \end{pmatrix}$	$\mathbf{U}_2=\begin{pmatrix} .9860 & -.0106 \\ -.0106 & 1.0130 \end{pmatrix}$	$\mathbf{R}_2=\begin{pmatrix} 1.0000 & -.0015 \\ .0015 & 1.0000 \end{pmatrix}$

Table 2

Force	F	U	R
T=26.7 N:	$\mathbf{F}_1=\begin{pmatrix} 1.0252 & .0108 \\ .0076 & .9768 \end{pmatrix}$	$\mathbf{U}_1=\begin{pmatrix} 1.0252 & .0092 \\ .0092 & .9768 \end{pmatrix}$	$\mathbf{R}_1=\begin{pmatrix} 1.0000 & .0016 \\ -.0016 & 1.0000 \end{pmatrix}$
	$\mathbf{F}_2=\begin{pmatrix} .9704 & -.0085 \\ -.0092 & 1.0320 \end{pmatrix}$	$\mathbf{U}_2=\begin{pmatrix} .9704 & -.0089 \\ -.0089 & 1.0320 \end{pmatrix}$	$\mathbf{R}_2=\begin{pmatrix} 1.0000 & .0003 \\ -.0003 & 1.0000 \end{pmatrix}$
T=35.6 N:	$\mathbf{F}_1=\begin{pmatrix} 1.0216 & .0099 \\ .0070 & .9811 \end{pmatrix}$	$\mathbf{U}_1=\begin{pmatrix} 1.0215 & .0085 \\ .0085 & .9812 \end{pmatrix}$	$\mathbf{R}_1=\begin{pmatrix} 1.0000 & .0014 \\ -.0014 & 1.0000 \end{pmatrix}$
	$\mathbf{F}_2=\begin{pmatrix} .9906 & -.0009 \\ -.0026 & 1.0106 \end{pmatrix}$	$\mathbf{U}_2=\begin{pmatrix} .9906 & -.0018 \\ -.0018 & 1.0106 \end{pmatrix}$	$\mathbf{R}_2=\begin{pmatrix} 1.0000 & .0009 \\ -.0009 & 1.0000 \end{pmatrix}$

deformations in the appropriate dead-loading device. Suppose also that these deformations are each homogeneous, as indicated in the experiments, although this is not really essential to the argument. If $\mathbf{y}^* = \mathbf{F}^*\mathbf{x}$ is one of these deformations corresponding to the applied tractions $T\mathbf{e}_1$ and $T\mathbf{e}_2$, then $\mathbf{y}^*$ satisfies

$$E[\mathbf{y}^*] \leq E[\mathbf{y}] \tag{11}$$

where $E[\mathbf{y}]$ is defined in (9).

Using the divergence theorem on the second term in (9) we get

$$E[\mathbf{y}] = \int_R (\varphi(\nabla\mathbf{y}(\mathbf{x}))d\mathbf{x} - \mathbf{T}\cdot\nabla(\mathbf{x}))d\mathbf{x}. \tag{12}$$

In particular,

$$E[\mathbf{y}^*] = \int_R (\varphi(\mathbf{F}^*) - \mathbf{T}\cdot\mathbf{F}^*)d\mathbf{x}. \tag{13}$$

As mentioned above, the symmetry group of the cloth used in the experiments contains the group $\mathcal{G} = \{\mathbf{H}(\pi/2), \mathbf{H}(\pi), \mathbf{H}(3\pi/2), \mathbf{1}\}$. Hence, combining this symmetry with the condition of frame indifference, we have

$$\varphi(\mathbf{HFH}^T) = \varphi(\mathbf{F}) \quad \text{for all } \mathbf{H} \in \mathcal{G} \tag{14}$$

and for all admissible $\mathbf{F}$. Generally, the term $-\mathbf{T}\cdot\mathbf{F}$ has no particular symmetry under $\mathbf{F} \to \mathbf{HFH}^T$, except in the special case $T_1 = T_2$, in which case

$$\mathbf{T}\cdot\mathbf{HFH}^T = T_1\mathbf{1}\cdot\mathbf{HFH}^T = \mathbf{T}\cdot\mathbf{F}. \tag{15}$$

Hence, in the equibiaxial case,

$$E[\mathbf{y}^*] = E[\hat{\mathbf{y}}],\ \hat{\mathbf{y}}(x) = \mathbf{HF}^*\mathbf{H}^T\mathbf{x}. \tag{16}$$

Now the deformation $\hat{\mathbf{y}}$ may or may not coincide with $\mathbf{y}^*$. Of course, $\mathbf{H}(\pi)\mathbf{FH}(\pi)^T = \mathbf{F}$ for all 2×2 tensors $\mathbf{F}$. Generally, $\mathbf{H}(\pi/2)\mathbf{F}^*\mathbf{H}(\pi/2)^T \neq \mathbf{F}^*$ and we certainly expect these to be different in a highly nonlinear material like cloth. The other symmetries give nothing new, and a deeper analysis shows that the symmetry-induced instability just analyzed is the only one expected.

If $\mathbf{F}^*$ has the form

$$\begin{pmatrix} F_{11} & F_{12} \\ F_{21} & F_{22} \end{pmatrix} \tag{17}$$

in an orthonormal basis, then $\mathbf{H}(\pi/2)\mathbf{F}^*\mathbf{H}(\pi/2)^T$ has the form

$$\begin{pmatrix} F_{22} & -F_{21} \\ -F_{12} & F_{11} \end{pmatrix} \tag{18}$$

in the same basis. Referring to the results in Section 4, we can see that the pairs of deformation gradients in the equibiaxial case are related approximately by (17) and (18).

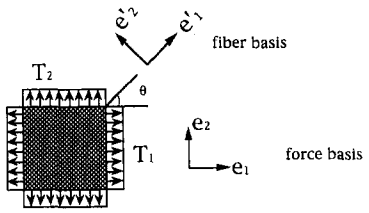

Fig. 6 Definitions of the force and fiber bases

It is often expected that a symmetry-induced nonuniqueness, such as the one analyzed here, has as its origins a bifurcation from a more symmetric deformation, which might occur at some different equibiaxial stress. No such bifurcation was detected in any of the tests in the range of loading suitable for the machine.

6 Strain-Energy Function in Inextensible Fiber Case

We have assumed that the strain energy of the cloth is a function of deformation gradient $\mathbf{F}$. In the general orthotropic case, this function depends on several invariants. We want to simplify this strain-energy function by using some available information. In previous work on similar materials by Pipkin and Rivlin (Pipkin, 1974 and 1987; Pipkin and Rivlin, 1963; Rivlin, 1955), the fibers have been treated as inextensible. In order to check this assumption in our material, let $\mathbf{e}'_1$, $\mathbf{e}'_2$ be an orthonormal basis along the fibers of the cloth in the undistorted configuration R (see Fig. 6). We assume that the tensor $\mathbf{C}$ has the following form:

$$\mathbf{C} = \mathbf{F}^T\mathbf{F} = \begin{pmatrix} C_{11} & C_{12} \\ C_{12} & C_{22} \end{pmatrix} \tag{19}$$

in the $\mathbf{e}'_1$, $\mathbf{e}'_2$ basis. It is convenient to use the basis $\mathbf{e}'_1$, $\mathbf{e}'_2$ for the derivation of the strain energy, since the argument of this function assumes a simple form in this basis.

We measured C_{11} and C_{22} when different biaxial loads were applied. The results indicate that the assumption of inextensibility is fairly reasonable (see the data in the last two columns of Tables 3 and 4), although the extension in the fiber directions was larger than the typical scatter of $\|\mathbf{F}\|$. Our observations suggested that the origin of this slight extensibility was due mainly to the bending of the fibers of the cloth. Since these fibers were forced to pass over and under each other due to the weave of the cloth, there was noticeable bending of the fibers when the tension was applied.

Under the inextensible assumption for the fibers, we have

$$C_{11} = F_{11}^2 + F_{21}^2 = 1, \tag{20}$$

and

$$C_{22} = F_{12}^2 + F_{22}^2 = 1. \tag{21}$$

Thus the strain-energy function depends only upon C_{12}. According to (20) and (21) we have, in the basis $(\mathbf{e}'_1, \mathbf{e}'_2)$,

$$\mathbf{F} = \begin{pmatrix} \cos\alpha & \sin\beta \\ \sin\alpha & \cos\beta \end{pmatrix}. \tag{22}$$

Then

$$\mathbf{C} = \mathbf{F}^T\mathbf{F} = \begin{pmatrix} 1 & \sin(\alpha+\beta) \\ \sin(\alpha+\beta) & 1 \end{pmatrix}. \tag{23}$$

Note that $\alpha + \beta$ is the angle change experienced by the originally orthogonal fibers during deformation. Let us assume that the strain-energy function has the following form:

$$\varphi = \phi(C_{12}), \quad -1 < \mathbf{C}_{12} < 1. \tag{24}$$

We define the total potential energy as in (9), which has the alternative form (12). Using $(24)_2$ we assume $|\alpha + \beta| < 90$ deg, which has the geometric interpretation of forbidding the fibers to become parallel.

A necessary and sufficient condition that a homogeneous deformation $\mathbf{y}(\mathbf{x}) = \mathbf{F}\mathbf{x}$ minimize the total potential energy is that it minimizes the integrand

$$\phi - \mathbf{F}\cdot\mathbf{T}. \tag{25}$$

Under the test machine (force) basis $\mathbf{e}_1$ and $\mathbf{e}_2$ (see Fig. 6), the expression for $\mathbf{T}$ in (25) is

$$\mathbf{T} = \sum_{i=1}^{2} T_i \mathbf{e}_i \otimes \mathbf{e}_i, \tag{26}$$

where $T_i > 0$. Let θ represent the angle between the fiber direction and the force direction (as shown in Fig. 6). In order to bring out the dependence on θ we write the expression (26) in the $\mathbf{e}'_1$ and $\mathbf{e}'_2$ basis, which gives

$$\mathbf{T} = \begin{pmatrix} T_1\cos^2\theta + T_2\sin^2\theta & (T_2 - T_1)\sin\theta\cos\theta \\ (T_2 - T_1)\sin\theta\cos\theta & T_2\cos^2\theta + T_1\sin^2\theta \end{pmatrix}. \tag{27}$$

Then we have

$$\begin{aligned} E := \phi - \mathbf{F}\cdot\mathbf{T} = \phi(\sin(\alpha+\beta)) \\ -(T_1\cos^2\theta + T_2\sin^2\theta)\cos\alpha \\ -(T_1\sin^2\theta + T_2\cos^2\theta)\cos\beta \\ -(T_2 - T_1)\sin\theta\cos\theta(\sin\alpha + \sin\beta). \end{aligned} \tag{28}$$

In order to discuss the stability of the deformation, we study the formula (28). If (α^*, β^*) is a local minimizer, then

$$\left.\frac{\partial E}{\partial\alpha}\right|_{\alpha^*,\beta^*} = \left.\frac{\partial E}{\partial\beta}\right|_{\alpha^*,\beta^*} = 0. \tag{29}$$

These give two equations for the determination of α^* and β^* which can be put in the forms

$$\begin{aligned} (T_1\cos^2\theta + T_2\sin^2\theta)\sin\alpha^* \\ +(T_1 - T_2)\sin\theta\cos\theta\cos\alpha^* \\ = (T_2\cos^2\theta + T_1\sin^2\theta)\sin\beta^* \\ +(T_1 - T_2)\sin\theta\cos\theta\cos\beta^* \end{aligned} \tag{30}$$

$$\phi'(\sin(\alpha^* + \beta^*)) = \frac{-(T_1\cos^2\theta + T_2\sin^2\theta)\sin\alpha^* + (T_2 - T_1)\sin\theta\cos\theta\cos\alpha^*}{\cos(\alpha^* + \beta^*)}. \tag{31}$$

The first of these conditions is a universal relation, expressing the fact that $\mathbf{T}\mathbf{F}^{*\mathrm{T}}$ is symmetric. This condition effectively determines the rigid rotation of the specimen.

If we let

$$A = \frac{\partial^2 E}{\partial\alpha^2}, \quad B = \frac{\partial^2 E}{\partial\alpha\partial\beta}, \quad C = \frac{\partial^2 E}{\partial\beta^2},$$

sufficient conditions for the potential energy E to have a local minimum at (α^*, β^*) are (29) and

$$B^2 - AC|_{\alpha^*,\beta^*} < 0, \tag{32}$$

$$A|_{\alpha^*,\beta^*} > 0. \tag{33}$$

Substituting A, B, and C into (32) we get the following condition for local stability:

$$\phi'' J_2 > \frac{J_1 J_2 - J_3 - J_4}{\cos^2(\alpha^* + \beta^*)} \tag{34}$$

where

$$\begin{aligned} J_1 = \phi'\sin(\alpha^* + \beta^*) \\ = \tan(\alpha^* + \beta^*)\big(-(T_1\cos^2\theta + T_2\sin^2\theta)\sin\alpha^* \\ +(T_2 - T_1)\sin\theta\cos\theta\cos\alpha^*\big), \end{aligned}$$

$$\begin{aligned} J_2 = (T_1\sin^2\theta + T_2\cos^2\theta)\cos\beta^* \\ +(T_2 - T_1)\sin\theta\cos\theta\sin\beta^* \\ +(T_1\cos^2\theta + T_2\sin^2\theta)\cos\alpha^* \\ +(T_2 - T_1)\sin\theta\cos\theta\sin\alpha^*, \end{aligned}$$

$$\begin{aligned} J_3 = (T_2 - T_1)\sin\theta\cos\theta \\ \times\big[(T_1\cos^2\theta + T_2\sin^2\theta)\cos\alpha^*\sin\beta^* \end{aligned}$$

Table 3 θ = 22.5 deg

Force (N)		C_{11}	C_{22}
T_1	T_2		
26.7	17.8	0.9999	0.9955
26.7	26.7	0.9984	1.0009
35.6	26.7	1.0017	1.0003
35.6	35.6	0.9991	1.0048
26.7	35.6	0.9996	1.0088
26.7	26.7	0.9998	1.0040
17.8	26.7	1.0004	1.0086
17.8	26.7	1.0006	1.0089
26.7	26.7	0.9994	1.0040
26.7	35.6	1.0012	1.0087
35.6	35.6	1.0003	1.0060
35.6	26.7	0.9997	1.0011
26.7	26.7	1.0009	1.0027
26.7	17.8	1.0005	0.9984

Table 4 θ = 35 deg

Force (N)		C_{11}	C_{22}
T_1	T_2		
17.8	26.7	0.9960	0.9997
26.7	26.7	0.9988	1.0022
26.7	35.6	0.9944	1.0018
35.6	35.6	0.9977	1.0048
35.6	26.7	1.0040	1.0027
26.7	26.7	1.0019	1.0034
26.7	17.8	1.0060	1.0016
26.7	17.8	1.0049	0.9992
26.7	26.7	1.0041	1.0026
35.6	26.7	1.0042	1.0031
35.6	35.6	1.0010	1.0053
26.7	35.6	0.9964	1.1132
26.7	26.7	0.9983	1.0047
17.8	26.7	0.9926	1.0027

$$+\left(T_1 \sin^2\theta + T_2 \cos^2\theta\right)\sin\alpha^* \cos\beta^*$$
$$+(T_2 - T_1)\sin\theta\cos\theta\sin\alpha^*\sin\beta^*\Big],$$
$$J_4 = \left(T_1\cos^2\theta + T_2\sin^2\theta\right)$$
$$\times\left(T_1\sin^2\theta + T_2\cos^2\theta\right)\cos\alpha^*\cos\beta^*.$$

Similarly, substituting A into (33) and using (31), we have

$$\phi'' > \frac{-\left(T_1\cos^2\theta + T_2\sin^2\theta\right)(\tan(\alpha^*+\beta^*)\sin\alpha^* + \cos\alpha^*)}{\cos^2(\alpha^*+\beta^*)} + \frac{(T_2 - T_1)\sin\theta\cos\theta(\tan(\alpha^*+\beta^*)\cos\alpha^* - \sin\alpha^*)}{\cos^2(\alpha^*+\beta^*)}. \tag{35}$$

Hence, in the case $J_2 > 0$ (which is the case in all of our experiments) sufficient conditions for stability represent a simple lower bound on ϕ'', either (34) or (35), which depends only on the load and the deformation. These conditions are necessary if equality is allowed.

Now let us specialize to the situation of $T_1 = T_2 = :T > 0$. In this case (30) becomes

$$\sin\alpha^* = \sin\beta^*. \tag{36}$$

Using $|\alpha + \beta| < 90$ deg we get from (36)

$$\alpha^* = \beta^* = :\gamma. \tag{37}$$

The conditions (34) and (35) in the equibiaxial case reduce to the following forms:

$$\phi'' > -\frac{T(2\tan 2\gamma \sin\gamma + \cos\gamma)}{2\cos^2 2\gamma}, \tag{38}$$

and

$$\phi'' > -\frac{T(\cos\gamma + \tan 2\gamma \sin\gamma)}{\cos^2 2\gamma}. \tag{39}$$

According to (22) and (37), the locally stable deformation gradient has the following form:

$$\mathbf{F} = \begin{pmatrix} \cos\gamma & \sin\gamma \\ \sin\gamma & \cos\gamma \end{pmatrix}. \tag{40}$$

At the same time, the total potential energy function becomes

$$E = \phi - \mathbf{F}\cdot\mathbf{T} = \phi(\sin 2\gamma) - 2T\cos\gamma. \tag{41}$$

If we change γ to $-\gamma$, the total potential energy will stay the same. This change in the sign of γ is equivalent to the symmetry transformation $\mathbf{H}(n\pi/2)$, where n is odd integer. The resulting deformation gradient (40) will change to the form

$$\mathbf{F} = \begin{pmatrix} \cos\gamma & -\sin\gamma \\ -\sin\gamma & \cos\gamma \end{pmatrix}. \tag{42}$$

Now let us transform (40) and (42) into the force basis. We get in the basis $(\mathbf{e}_1, \mathbf{e}_2)$

$$\mathbf{F} = \begin{pmatrix} \cos\gamma - 2\sin\gamma\sin\theta\cos\theta & -\cos 2\theta\sin\gamma \\ -\sin 2\theta\sin\gamma & \cos\gamma + 2\sin\gamma\sin\theta\cos\theta \end{pmatrix} \tag{43}$$

and

$$\mathbf{F} = \begin{pmatrix} \cos\gamma + 2\sin\gamma\sin\theta\cos\theta & \cos 2\theta\sin\gamma \\ \sin 2\theta\sin\gamma & \cos\gamma - 2\sin\gamma\sin\theta\cos\theta \end{pmatrix}. \tag{44}$$

If we compare (43) and (44) with Table 1 and Table 2, we find that the deformation gradients in these tables have the forms of (43) and (44).

Further, using the assumption of inextensible cords and the stability conditions given above, in Section 7 we can restrict the possible forms of the energy function by measuring the angles α and β of the deformed fibers.

7 Evaluation of the Strain-Energy Function

In order to find the strain-energy function, several experiments were carried out in our biaxial machine. In these experiments, pieces of cloth which were cut at $\theta = 22.5$ deg and $\theta = 35$ deg were tested under different loads and the deformations were recorded, respectively. To reveal the nature of $d\phi/dC_{12}$ versus C_{12} we decided to take the average values of data, bearing in mind the scatter discussed at the beginning of Section 4. Besides C_{12} and $d\phi/dC_{12}$, the right-hand sides of inequalities (34) and (35) were also calculated for the purpose of checking the stability. From the direct measurements of the deformation gradient $\mathbf{F}$, we can compute C_{12} and, from Eq. (31), ϕ' (see Table 5 for these measured data).

$d\phi/dC_{12}$ versus C_{12} was plotted as shown in Fig. 5, and it was found that all the points in the central part belonged to the equibiaxial load, i.e., $T_1 = T_2$. Among those points, the positive $d\phi/dC_{12}$ points correspond to the negative C_{12} and the negative $d\phi/dC_{12}$ points corresponds to the positive C_{12}.

According to the experimental results, there are several possible strain-energy functions which are consistent with the experimental data. Since the strain-energy function is an even function of C_{12} by (7), we only need to discuss it for $C_{12} \geq 0$.

Hypothesis 1 is shown in Fig. 8. From this assumption, the strain-energy function ϕ has the shape as shown in Fig. 9.

Let us discuss the stability for an equibiaxial load case. Equation (29) is satisfied at $\alpha = \beta = 0$. The second derivative tests (conditions (38) and (39)) have the forms

$$\phi'' > -\frac{T}{2} \tag{45}$$

and

Table 5

Force (N)		C_{12}	$\frac{d\phi}{dC_{12}}$
T_1	T_2		
24.5	15.5	0.1204	1.9656
24.5	24.5	0.0219	-0.1731
33.4	24.5	0.0881	1.8623
33.4	33.4	0.0247	-0.2700
24.5	33.4	-0.0734	-1.8548
24.5	24.5	-0.0227	0.3560
15.5	24.5	-0.1231	-1.8783
33.4	33.4	-0.0156	0.3653
15.5	28.9	-0.1888	-2.6175
28.9	15.5	0.1851	2.6896
33.4	20.0	0.1808	2.3652
20.0	33.4	-0.1435	-2.7514
26.7	31.2	-0.0436	-0.7779
15.5	20.0	-0.0503	-1.0756
24.5	20.0	0.0530	0.9990
28.9	24.5	0.0456	1.0075
20.0	15.5	0.0553	1.0920

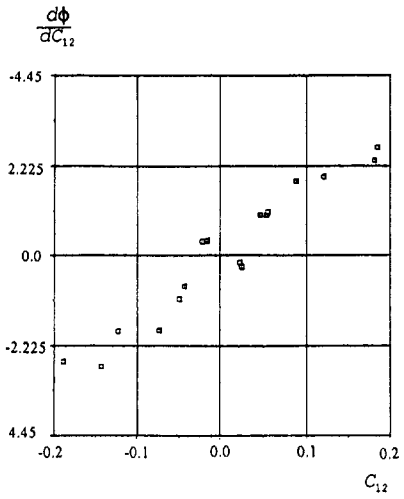

Fig. 7 $d\phi / dC_{12}$ versus C_{12} from Experimental data, Table 5

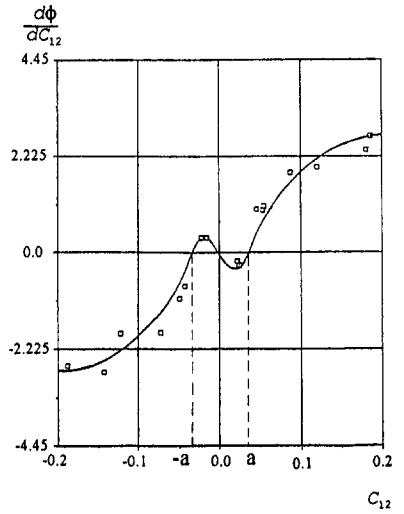

Fig. 8 $d\phi / dC_{12}$ versus C_{12} corresponding to Hypothesis 1

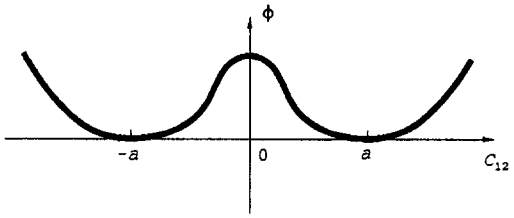

Fig. 9 Strain-energy function corresponding to Hypothesis 1

$$\phi'' > -T \tag{46}$$

These conditions are inconclusive because the precise value of $\phi''(0)$ is not known. However, Hypothesis 1 with ϕ'' sufficiently negative near $C_{12} = 0$ would rule out a locally stable equilibrium near $C_{12} = 0$, consistent with experiments. Of course, it must be appreciated that this hypothesis cannot be applied to the situation of zero load, because the natural state $\alpha = \beta = 0$ appears to be stable under zero load.

In order to discuss the possible global minima, let us rewrite (41) in the following form:

$$E = \phi(C_{12}) - 2T\cos\left(\frac{1}{2}\sin^{-1}C_{12}\right). \tag{47}$$

Subtracting $2T\cos(1/2\sin^{-1}C_{12})$ from Fig. 9 yields Fig. 10.

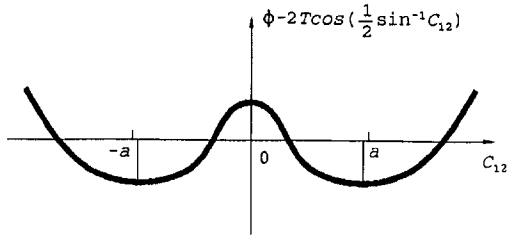

Fig. 10 The function $\phi(C_{12})-2T\cos\left(1/2\sin^{-1}C_{12}\right)$ under Hypothesis 1

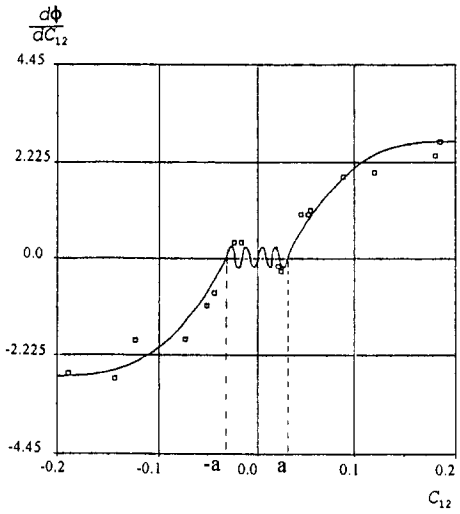

Fig. 11 $d\phi / dC_{12}$ versus C_{12} corresponding to Hypothesis 2

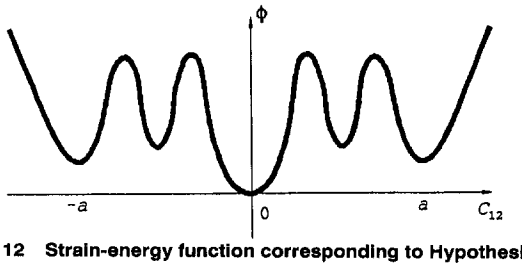

Fig. 12 Strain-energy function corresponding to Hypothesis 2

Since $2T\cos(1/2\sin^{-1}C_{12})$ is concave and almost flat between $C_{12} = 0$ and $C_{12} = a$, a global minimum is expected just to the left of $C_{12} = a$, as shown in Fig. 10. Therefore, Hypothesis 1 is at least consistent with all the measured data.

Hypothesis 2 is based upon the curve of $d\phi/dC_{12}$ versus C_{12} as shown in the Fig. 11. The strain energy function has some wells as shown in Fig. 12. In this case we assume that the well at $C_{12} = 0$ has the lowest value. Checking the function (41) at $C_{12} = 0$ gives

$$E = \phi(0) - 2T = -2T. \tag{48}$$

This is the global minimum. Hence, if Hypothesis 2 was the case, we expect to have observed deformation $\alpha = \beta = 0$, particularly during loading with $T_1 = T_2$ beginning at the natural state. Since we did not observe $\alpha = \beta = 0$ in any experiment, we conclude that Hypothesis 2 is not the case.

Hypothesis 3 is also based upon a similar curve of $d\phi/dC_{12}$ versus C_{12} as that shown in the Fig. 11 for Hypothesis 2, but the shape of the strain energy function is as shown in Fig. 13. The difference from Hypothesis 2 is that the two outside wells have lower values than those inside.

Similarly, subtracting $2T\cos(1/2\sin^{-1}C_{12})$ from Fig. 13 yields Fig. 14. Depending on the relative heights of the inside wells relative to the two outside wells, we can retain the

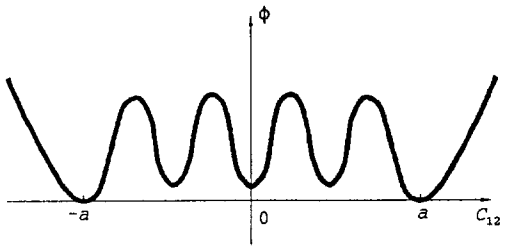

Fig. 13 Strain-energy function corresponding to Hypothesis 3

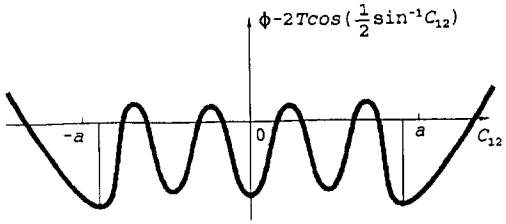

Fig. 14 The function $\phi(C_{12}) - 2T\cos\left(1/2\sin^{-1}C_{12}\right)$ under Hypothesis 3

feature that there are global minima near $\pm a$. In addition, there remain several local minimizers in the interval $(-a, a)$.

From the above discussion, we see that Hypothesis 1 and Hypothesis 3 are consistent with our experiments and obviously there are many other possibilities.

Since it may not be possible to observe any local minimizers, it is not known how many potential wells lie between $C_{12} = -a$ and $C_{12} = a$. From experience with cloth-type materials under no loads, we know that cloth has many stable (or metastable) deformed configurations. In fact, when the cloth was unloaded along an equibiaxial loading path from an unsymmetrical state, it remained unsymmetrical even under zero load. It is thus conceivable that the cloth is modeled by a ϕ with many potential wells between $-a$ and $+a$. It is interesting to note that the point $C_{12} = 0$ would become stable for sufficiently large loads under any of the hypotheses 1–3. This was not observed in our limited loading range.

Acknowledgment

The authors thank ONR (N00014-91-J-4034), AFOSR (AFOSR-91-0301), NSF (NSF/DMS-8718881) and ARO (28987 MA/27063 MA-SM) for supporting this work.

References

Ball, J. M., and Schaeffer, D. G., 1983, "Bifurcation and Stability of Homogeneous Equilibrium Configurations of an Elastic Body under Dead-Load Tractions," *Mathematical Proceeding Cambridge Philosophical Society*, Vol. 94, pp. 315–339.

Chadwick, P., 1976, *Continuum Mechanics: Concise theory and problems*, George Allen & Unwin, London, pp. 22, 138.

Chen, Y. C., 1987, "Stability of Homogeneous Deformations of an Incompressible Elastic Body under Dead-Load Surface Tractions," *Journal of Elasticity*, Vol. 17, pp. 223–248.

Kearsley, E. A., 1986, "Asymmetric Stretching of a Symmetrically Loaded Elastic Sheet," *International Journal of Solids and Structures*, Vol. 22, pp. 111–119.

MacSithigh, G. P., 1986, "Energy-Minimal Finite Deformations of a Symmetrically Loaded Elastic Sheet," *Quarterly Journal of Mechanics and Applied Mathematics*, Vol. 39, pp. 111–123.

Pipkin, A. C., 1974, "Generalized Plane Deformations of Ideal Fiber-Reinforced Materials," *Quarterly Applied Mathematics*, Vol. 32, pp. 253–263.

Pipkin, A. C., 1974, "Infinitesimal Plane Wrinkling of Inextensible Networks," *Journal of Elasticity*, Vol. 17, pp. 35–52.

Pipkin, A. C., and Rivlin, R. S., 1963, "Minimum-Weight Design for Pressure Vessels Reinforced with Inextensible Fibers," ASME JOURNAL OF APPLIED MECHANICS, Vol. 30, pp. 103–108.

Rivlin, R. S., 1955, "Plane Strain of a Net Formed by Inextensible Cords," *Journal of Rational Mechanics and Analysis*, Vol. 4, pp. 951–974.

Rivlin, R. S., 1948, "Large Elastic Deformations of Isotropic Materials II: Some Uniqueness Theorems for Pure Homogeneous Deformation," *Philosophical Transactions, Royal Society of Lond.*, Vol. A240, pp. 491–508.

Rivlin, R. S., 1974, "Stability of Pure Homogeneous Deformation of an Elastic Cube under Dead Loading," *Quarterly Applied Mechanics*, Vol. 32, pp. 265–271.

Rivlin, R. S., and Saunders, D. W., 1951, "Large Elastic Deformations of Isotropic Materials VII: Experiments on the Deformation of Rubber," *Philosophical Transactions, Royal Society of Lond.*, Vol. A243, pp. 251–288.

Treloar, L. R. G., 1948, "Stress and Birefringence in Rubber Subjected to General Homogeneous Strain," *Proceedings, Physics Society*, Vol. 60, pp. 135–144.

Treloar, L. R. G., 1949, *Physics of Rubber Elasticity*, Oxford University Press, London, pp. 116.